

## SUPPLEMENTARY MATERIAL

### Optimal Decision Making in Neural Inhibition Models

Don van Ravenzwaaij, Han L. J. van der Maas, Eric-Jan Wagenmakers  
University of Amsterdam

Correspondence concerning this article should be addressed to:

Don van Ravenzwaaij  
University of Amsterdam, Department of Psychology  
Roetersstraat 15  
1018 WB Amsterdam, The Netherlands  
Ph: (+31) 20-525-8870  
E-mail should be sent to d.vanravenzwaaij@uva.nl.

This document contains supplementary material to van Ravenzwaaij, van der Maas, and Wagenmakers (2011).

#### Matched Accuracy LCA Simulation 1

The non-truncated LCA does not perform the same as the optimal DDM (see van Ravenzwaaij et al., 2011, section “LCA Simulation 1: Performance” and Figure 8). Specifically, the non-truncated LCA is slightly faster than the DDM at the cost of more errors. In this section we present additional simulations where the mean percentage correct of the non-truncated LCA is matched to the mean percentage correct of the DDM. The results are displayed in Figure 1. The figure shows how for matching accuracy (bottom panels), the DDM is faster than the non-truncated LCA for the whole range of values for decay and inhibition parameters  $k$  and  $w$  for all three levels of accuracy.

#### Higher Input LCA Simulation 1

Both the previous section and section “LCA Simulation 1: Performance” of van Ravenzwaaij et al. (2011) show a discrepancy in performance between the non-truncated LCA and the DDM for DDM drift rate  $v = 0.2$ . In this section, we show the same pattern of discrepancy for a DDM drift rate  $v = 0.3$ . The results are displayed in Figure 2. The figure shows the familiar discrepancy between the DDM and the non-truncated LCA for the whole range of values for decay and inhibition parameters  $k$  and  $w$  for all three levels of accuracy.

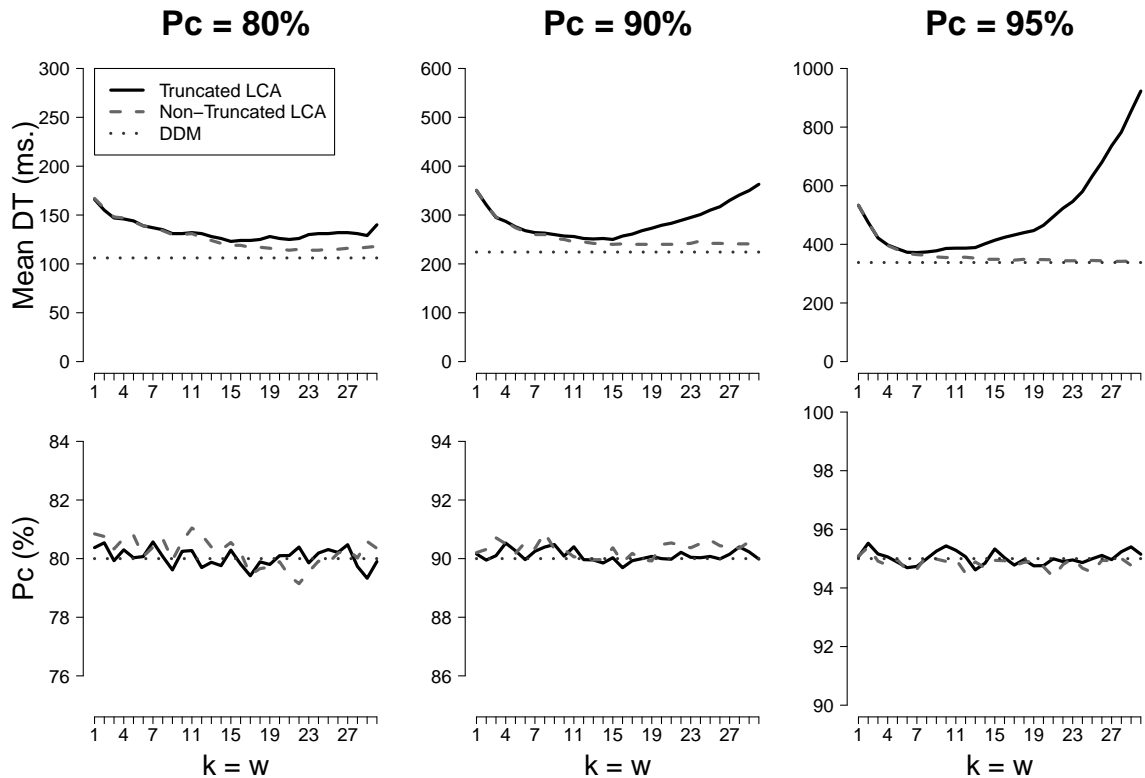


Figure 1. The DDM is faster than both versions of the LCA for matched accuracy. Simulation results for DDM drift rate  $v = 0.2$ . Top panels: mean decision time. Bottom panels: percentage correct. DDM boundary separations were set to match mean percentage correct of 80% (left panels), 90% (middle panels), and 95% (right panels).

### Full DDM Estimates LCA Simulation 2

Full DDM parameter estimates for the LCA model may be found in Figure 3 (see section “LCA Simulation 2: Parameters” of van Ravenzwaaij et al., 2011 for more information).

In general, results for the full DDM are very similar to the results for the optimal DDM. For the truncated LCA, the negative biases for drift rate  $v$  and non-decision time  $T_{er}$  are now mostly picked up instead by a non-zero estimate for across-trial variability in drift rate  $\eta$  and range of the starting point  $s_z$ . The bias in across-trial variability in drift rate  $\eta$  may be explained by the fact that truncation leads the winning accumulator to level off at an asymptote. Due to the asymptote, RTs will increase, creating the illusion of a lower drift rate. Since this effect will only occur in trials where truncation takes place, the effect is picked up by the  $\eta$  parameter. Effects on the range of the starting point  $s_z$  are probably caused by discrepancy 2: the across-trial variability in boundary separation. The best approximate of this phenomenon in the diffusion model is a non-zero value for the range of the starting point  $s_z$ .

For the non-truncated LCA, all parameter estimates look quite good. There are

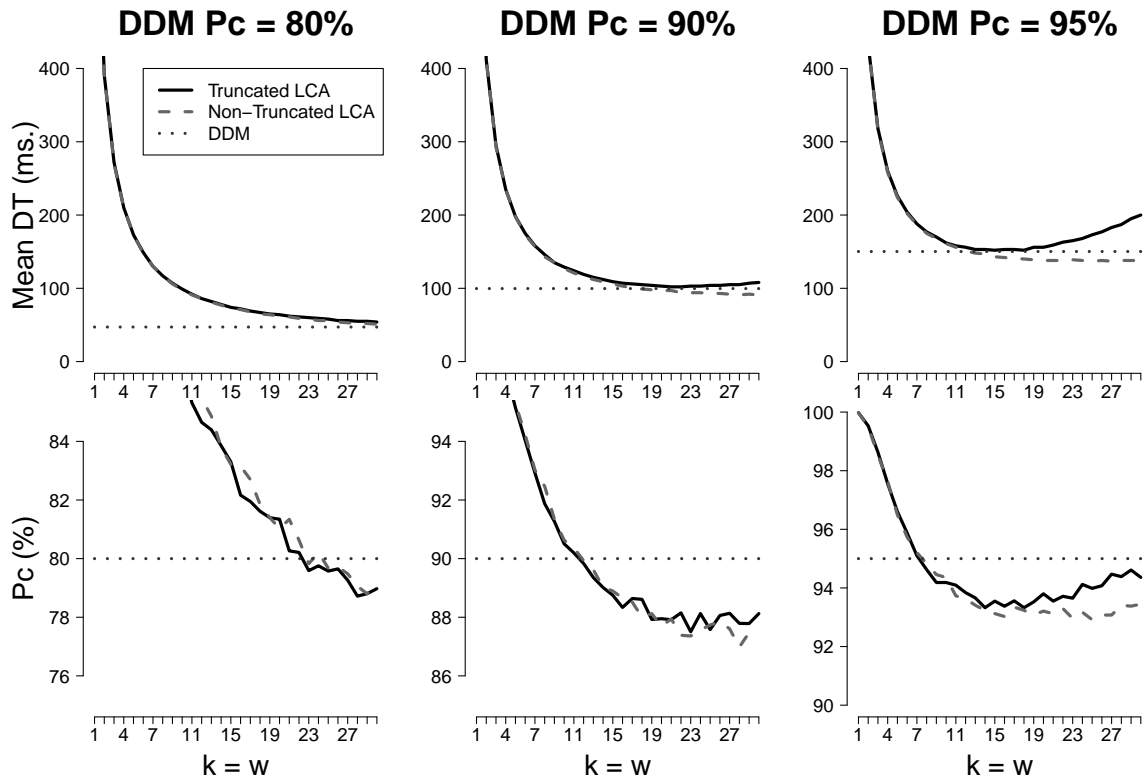


Figure 2. Simulation results for DDM drift rate  $v = 0.3$ . Top panels: mean decision time. Bottom panels: percentage correct. DDM boundary separations were set to match mean percentage correct of 80% (left panels), 90% (middle panels), and 95% (right panels).

slight non-zero estimates for some dispersion parameters for some parameter settings, but nothing systematic seems to be going on.

### Matched Accuracy FFI Simulation 1

The truncated FFI does not perform the same as the DDM (see section “FFI Simulation 1: Performance” of the full paper for more information). For corresponding parameter settings, the DDM is more accurate yet slightly slower. To be able to compare the models unambiguously, we have simulated both FFI and DDM data with a percentage correct of 95%. The resulting data is displayed in Figure 4. The figure shows how for the whole range of values for the input parameters, the DDM has a shorter mean decision time than the FFI.

### Full DDM Estimates FFI Simulation 2

Full DDM parameter estimates for the FFI model may be found in Figure 5 (see section “FFI Simulation 2: Parameters” of van Ravenzwaaij et al., 2011 for more information).

In general, results for the full DDM are very similar to the results for the optimal

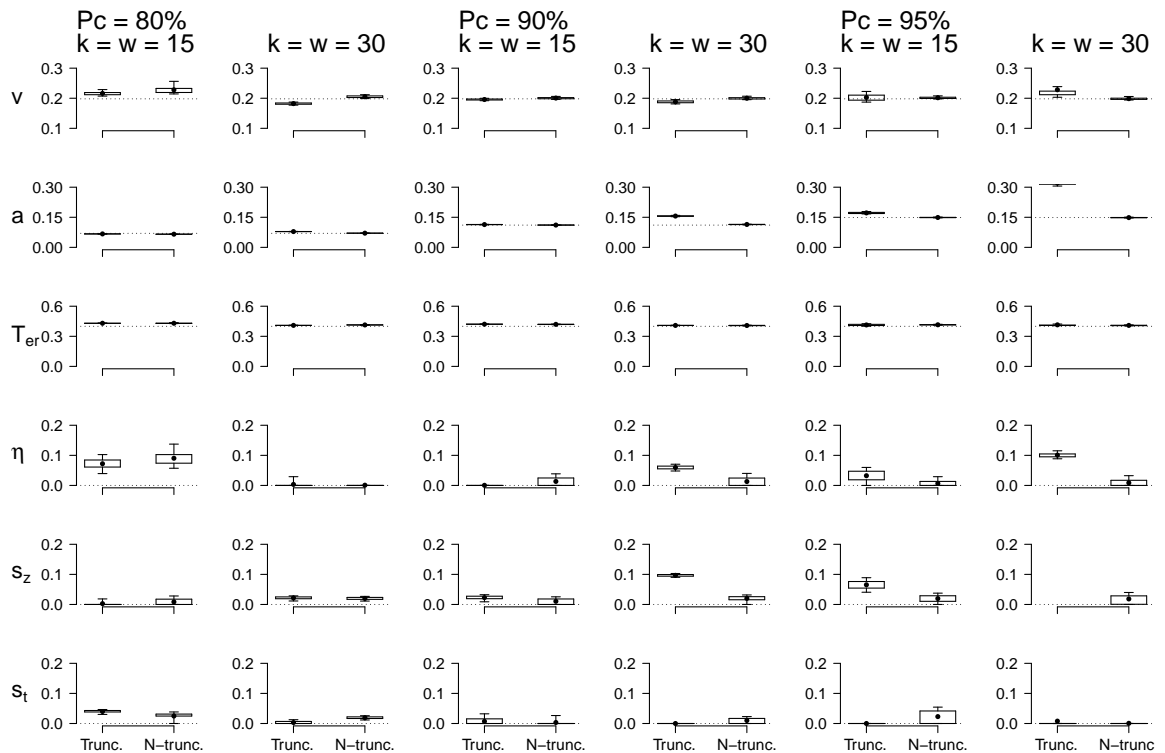


*Figure 3.* DDM estimates for LCA data. Dots represent the mean of the 1000 bootstrap parameter estimates, with boxes containing 50% and whiskers extending to 90% of these estimates. The left two columns represent data for a mean percentage correct of 80%, the middle two columns represent data for a mean percentage correct of 90%, and the right two columns represent data for a mean percentage correct of 95%. The three panel rows represent estimates for DDM parameters  $v$ ,  $a$ ,  $T_{er}$ ,  $\eta$ ,  $s_z$ , and  $s_t$ , respectively. For each panel, the left boxes represent the truncated LCA and the right boxes represent the non-truncated LCA.

DDM. For the truncated FFI, there are positive biases for across-trial variability in drift rate  $\eta$  and range of the non-decision time  $s_t$  in addition to the familiar biases for drift rate  $v$  and non-decision time  $T_{er}$ . However, these biases do not appear to be very systematic.

For the non-truncated FFI, all parameter estimates look very good.

### LCA Truncation with Starting Points Above Zero

An intuitive solution to the discrepancy of truncation in the LCA model would be to have both accumulators start above zero. This solution works nicely for the FFI model, because the dynamic of the accumulators stays the same irrespective of the starting point. In the LCA however, increasing the starting point to a point between zero and the response threshold  $Z$  does change the dynamic of the model; both accumulators start out strongly inhibiting each other. Figure 6 shows this dynamic for parameter values  $I_1 = 2.41$ ,  $I_2 = 1$ ,  $s = 0.33$ ,  $k = w = 10$ , and  $Z = 0.18$  (the response threshold corresponding to a percentage

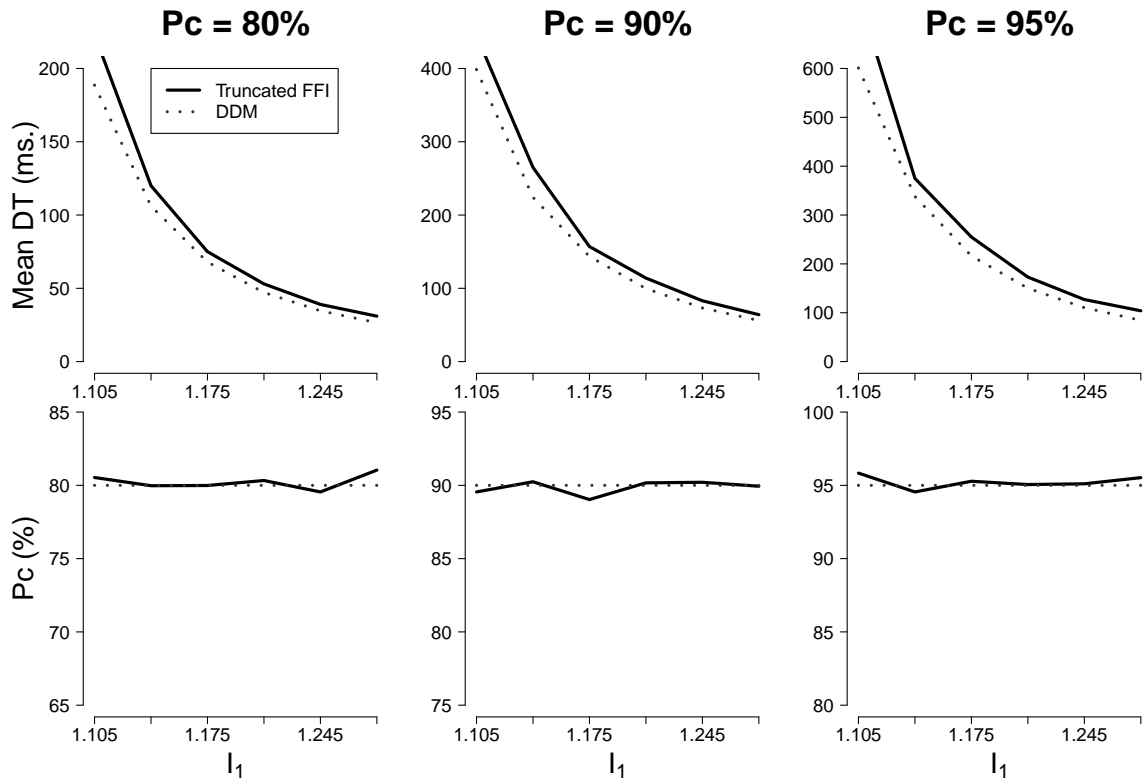
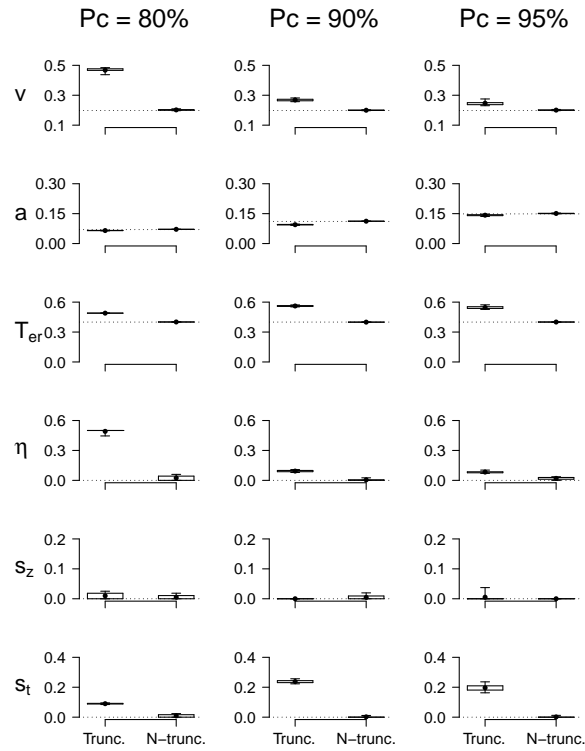


Figure 4. The DDM is faster than the truncated FFI for matched accuracy. Simulation results for DDM drift rates  $v = \{0.15, 0.20, \dots, 0.40\}$ . Top panels: mean decision time. Bottom panels: percentage correct. DDM boundary separations were set to match mean percentage correct of 80% (left panels), 90% (middle panels), and 95% (right panels).

correct of 90%).

Figure 6 shows that even when both accumulators start at three-quarters of the response threshold, the losing accumulator will still hit the zero boundary before a response is made. In this particular example, having a high starting point actually leads to the wrong answer (see bottom right panel). We have simulated 1000 trials for starting points at 0,  $0.25 \times Z$ ,  $0.50 \times Z$ , and  $0.75 \times Z$ . We found that truncation was necessary for 96.1%, 75.0%, 53.8%, and 34.3% for these starting points respectively. This means that even when the accumulators start at three quarters of the response threshold (so that they only need to travel a quarter of the distance of the regular LCA accumulators), there is still truncation of the losing accumulator in approximately one third of the trials.



*Figure 5.* DDM estimates for FFI data. Dots represent the mean of the 1000 bootstrap parameter estimates, with boxes containing 50% and whiskers extending to 90% of these estimates. The left, middle, and right columns represent data for a mean percentage correct of 80%, 90%, and 95%, respectively. The three panel rows represent estimates for DDM parameters  $v$ ,  $a$ ,  $T_{er}$ ,  $\eta$ ,  $s_z$ , and  $s_t$ , respectively. For each panel, the left boxes represent the truncated FFI and the right boxes represent the non-truncated FFI.

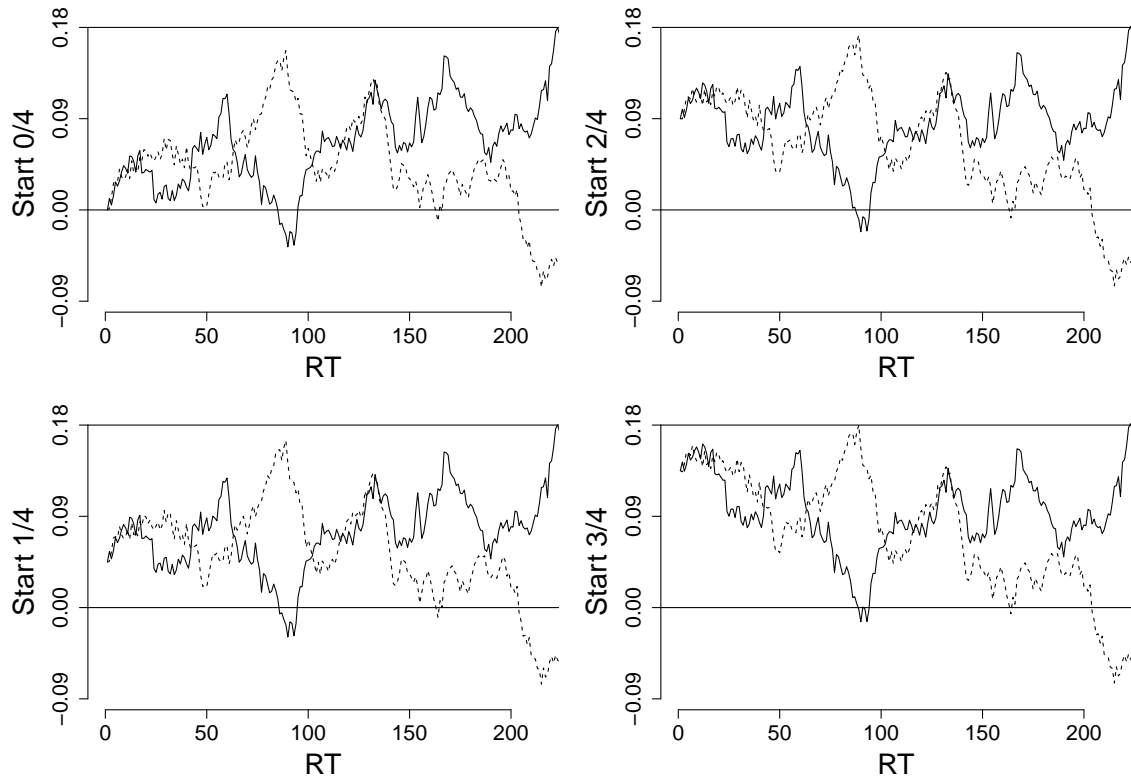


*Figure 6.* LCA accumulator dynamic with the same noise pattern for the accumulators in each panel, but a different starting point. The initial disparity between the four panels gradually disappears. Parameter values:  $I_1 = 2.41$ ,  $I_2 = 1$ ,  $s = 0.33$ ,  $k = w = 10$ , and  $Z = 0.18$ .

## References

- Matzke, D., & Wagenmakers, E.-J. (2009). Psychological interpretation of ex-Gaussian and shifted Wald parameters: A diffusion model analysis. *Psychonomic Bulletin & Review*, *16*, 798–817.
- van Ravenzwaaij, D., van der Maas, H. L. J., & Wagenmakers, E.-J. (2011). Optimal decision making in neural inhibition models. Manuscript submitted for publication.